



**HAL**  
open science

## Vibration prediction of rotating composite fan blades comprising viscoelastic damping treatments

Lucie Rouleau, Olivier de Smet, Jean-François Deü

► **To cite this version:**

Lucie Rouleau, Olivier de Smet, Jean-François Deü. Vibration prediction of rotating composite fan blades comprising viscoelastic damping treatments. *Journal of Sound and Vibration*, 2022, 536, pp.117135. 10.1016/j.jsv.2022.117135 . hal-04016963

**HAL Id: hal-04016963**

**<https://hal.science/hal-04016963v1>**

Submitted on 12 Jan 2024

**HAL** is a multi-disciplinary open access archive for the deposit and dissemination of scientific research documents, whether they are published or not. The documents may come from teaching and research institutions in France or abroad, or from public or private research centers.

L'archive ouverte pluridisciplinaire **HAL**, est destinée au dépôt et à la diffusion de documents scientifiques de niveau recherche, publiés ou non, émanant des établissements d'enseignement et de recherche français ou étrangers, des laboratoires publics ou privés.

# Vibration prediction of rotating composite fan blades comprising viscoelastic damping treatments

Lucie Rouleau,<sup>\*</sup> Olivier De Smet and Jean-François Deü<sup>\*</sup>

*Laboratoire de Mécanique des Structures et des Systèmes Couplés,  
Conservatoire national des arts et métiers,  
F 75003, Paris, France  
HESAM Université*

---

## Abstract

To reduce the risk of fatigue problems and flutter phenomena, the structural damping of turbomachinery components is increased by integrating constrained viscoelastic patches into rotating composite blades. However, the temperature, the frequency (of the vibration mode to be damped) and the rotation speed are all parameters which may affect significantly the efficiency of the viscoelastic damping treatment.

In the presented work, a numerical tool is developed to predict the structural damping of a dynamic rotating composite fan blade while varying the temperature and the rotation speed. This study is based on a finite element model of a fan disk sector equipped with constrained viscoelastic patches. This work will allow quantifying the influence of temperature and rotation speed on the efficiency of the passive damping treatment and contribute to the design of higher performing blades.

*Key words:* Rotating blade, Finite element method, Viscoelastic damping

---

## 1. Introduction

Advanced aircraft engines have to meet the increasing environmental regulatory requirements, leading to lightweight structures, which are more suscep-

---

<sup>\*</sup>Corresponding author

tible to excessive vibrations. To reduce the risk of fatigue problems and flutter  
5 phenomena, the structural damping of turbomachinery components has to be  
increased. This study concerns the vibration reduction in the low frequency  
range of a rotating composite fan blade of a turbojet engine by embedding  
constrained viscoelastic patches into the host structure. This passive damp-  
ing treatment relies on the characteristics of viscoelastic materials which allow  
10 energy dissipation. It has been successfully applied to many industrial applica-  
tions over the last decades.

One of the challenges in the integration of constrained viscoelastic patches into  
rotating composite blades is the frequency- and temperature-dependence of the  
mechanical properties of the viscoelastic material. Moreover, the amount of  
15 structural damping provided by the patches depends on the shear strain levels  
in the damping layer. Since the centrifugal force acting on the blade generates  
rotation-prestress, causing stiffening effects, the structure deforms less and so  
does the viscoelastic layer. Therefore, the temperature, the frequency (of the  
vibration mode to be damped) and the rotation speed are all parameters which  
20 may affect significantly the efficiency of the damping treatment. The design of  
higher performing blades requires a numerical tool to predict their dynamic be-  
haviour and estimate the influence of temperature and rotation speed on modal  
damping factors.

In the prediction of the dynamic behaviour of rotating composite blades, many  
25 papers can be found in the the literature [1, 2]. However, a limited number of  
studies concerns the dynamic behaviour of rotating structures with constrained  
viscoelastic layers. Most of them are limited to rotating plates [3, 4] or beams  
[5, 6], which do not account for the complex geometry and structure of cur-  
rent composite turbine blades [7]. In addition, the mechanical properties of the  
30 damping layer are often considered as constant [3, 4] even though the modulus  
of viscoelastic materials is known to be strongly frequency-dependent. In the  
aforementioned literature, parametric studies are performed to investigate the  
influence of the properties and dimensions of the constrained viscoelastic layer,  
and of the rotation speed on the modal damping of the rotating structure. The

35 influence of temperature seems to have never been studied, while fan blades are subjected to significant variations of temperature in operating conditions.

In the presented work, a numerical tool is developed to predict the structural damping of a dynamic rotating composite fan blade while varying both the temperature and the rotation speed. This study is based on a 3D finite element  
40 model of a fan disk sector equipped with constrained viscoelastic patches. The first goal of this study is to investigate the efficiency of the passive treatment in operation. The fan blade under study is on the outside of the engine, so it will undergo large temperature variations depending on the region where the aircraft is operating. Additionally, during a flight cycle, the fan blade will rotate at  
45 different angular speeds. The frequency- and the temperature-dependency of the viscoelastic material's properties is taken into account to evaluate the efficiency of the damping treatment at each operating point. The second goal of this work is to study the influence of the material selection on the efficiency of the damping treatment and to investigate the potential advantage of combining  
50 different viscoelastic materials.

The next section describes the finite element model of the blade disk sector, and the dynamic modelling of the rotating structure with embedded viscoelastic patches when subjected to harmonic excitation. Results are presented and discussed in the third section, and conclusions are given in the last section.

## 55 **2. Numerical model**

### *2.1. Description of the finite element model*

The structure under study is an assembly of a disk sector and a 3D woven carbon epoxy composite fan blade from the LEAP engine. Because of the complex geometry and the 3D-woven architecture, the structure is meshed by 3D  
60 finite elements (Figure 1). Each finite element of the blade has its own local coordinate system and is associated to a homogenised material behaviour, to account for the anisotropy of the woven composite [8].

The friction contact at the interface between the disk and the blade [9] is not

taken into account in this work. Instead, rigid elements are added into the finite  
65 element model to ensure the permanent contact between the disk and the blade.  
Two viscoelastic patches have been designed to mainly damp the first mode of  
vibration, which is the most critical for flutter. They are positioned on top  
of the extrado wall of the blade [7] (see Figure 1). Each viscoelastic patch  
is composed of a 0.3 mm thick viscoelastic layer and a 0.6 mm thick com-  
70 posite constraining layer. Two viscoelastic materials are used : material A  
for the viscoelastic patch 1 and material B for the viscoelastic patch 2. Both  
materials are thermo-rheologically simple, which means they respect the time-  
temperature superposition principle. This principle supposes an equivalence  
between time (or frequency) and temperature effects : viscoelastic properties  
75 measured at one temperature can be shifted along the time (or frequency) axis  
to obtain the viscoelastic properties at another temperature. For both mate-  
rials, the time-temperature superposition principle was applied to DMA mea-  
surements to obtain the storage modulus and the loss factor on the frequency  
range of investigation at any temperature comprised between  $-40^{\circ}\text{C}$  and  $70^{\circ}\text{C}$ .  
80 The temperature-dependent viscoelastic properties are plotted at two different  
frequencies (corresponding to the first and the fifth vibration mode of the struc-  
ture) in Figure 2. A complex, frequency- and temperature-dependent shear  
modulus  $G^*(f, T)$ , and a constant Poisson ratio are considered in this work for  
each viscoelastic material. To properly account for the shear behaviour in the  
85 damping layer, 20-node hexaedra are used to mesh the whole structure, leading  
to a finite element model of 838 000 degrees of freedom.  
Finally, cyclic symmetry boundary conditions are applied to the fan disk sec-  
tor [10] to account for the cyclo-symmetry geometry of the fan blade assembly.  
This study is focused on the zero-order harmonics so that the cyclic symme-  
90 try boundary conditions resume to symmetric boundary conditions, applied on  
the two sides of the disk connected to adjacent disk sectors. The structure is  
harmonically-excited by a point load on the blade, indicated on Figure 1.(b).  
This load point has been chosen to excite all the vibration modes on the fre-  
quency range of interest.

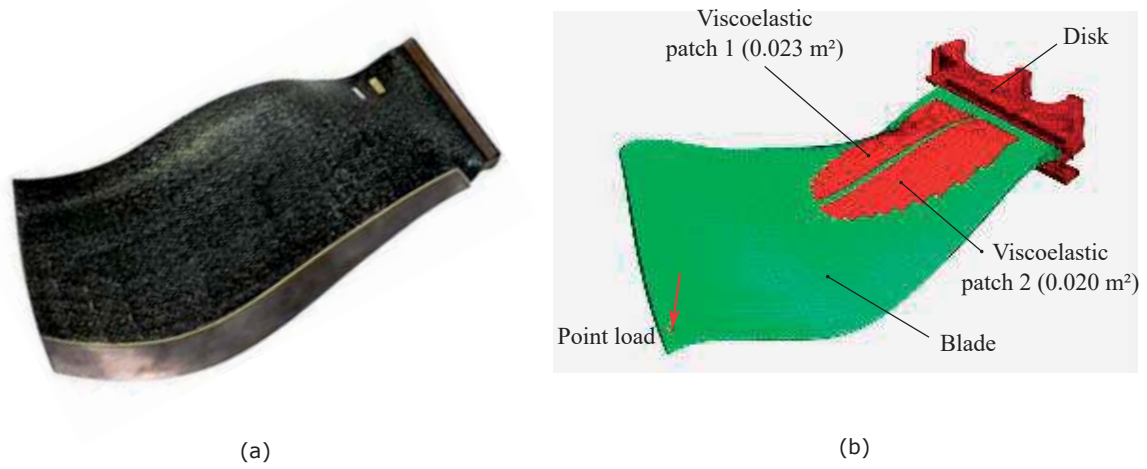


Figure 1: (a) 3D woven carbon epoxy composite fan blade and (b) finite element model of the fan disk sector with two viscoelastic patches.

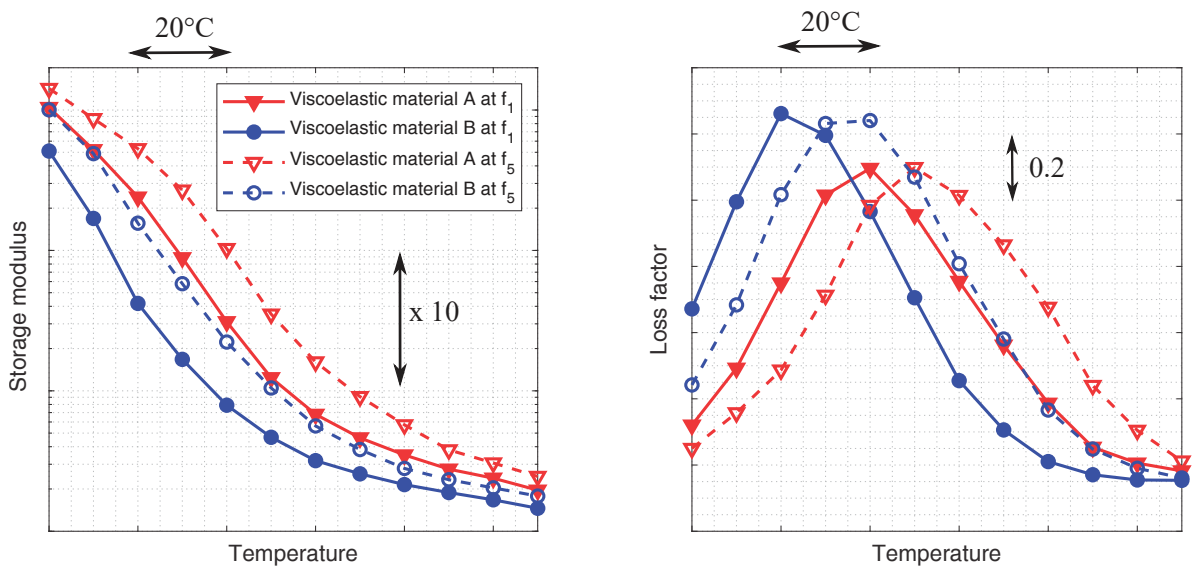


Figure 2: Temperature-dependent properties of viscoelastic materials A and B at two frequencies.

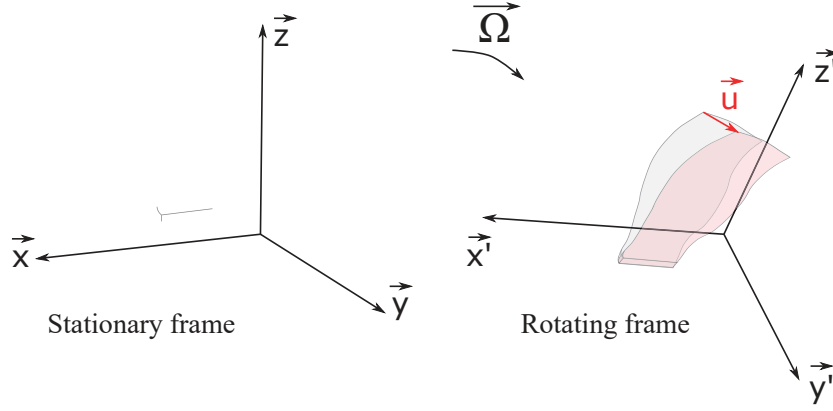


Figure 3: Stationary and rotating reference frame.

95 *2.2. Dynamic modelling*

Let us consider that the flexible fan blade is rotating at an arbitrary rotation  $\mathbf{\Omega} = [\Omega_x \quad \Omega_y \quad \Omega_z]^T$  with respect to the stationary frame (see Figure 3). The chosen reference configuration, in which the equations of motion are derived, is the rotating frame. In this reference configuration, the displacement between the undeformed and the deformed configuration is denoted  $\mathbf{u}(\mathbf{x}, t)$ , where  $\mathbf{x}$  is the coordinate vector of the undeformed structure in the reference configuration.

Using the finite element method, the displacement field can be approximated by:

$$\mathbf{u}(\mathbf{x}, t) = \mathbf{N}(\mathbf{x})\mathbf{U}(t) \quad (1)$$

where  $\mathbf{N}(\mathbf{x})$  is the matrix of shape functions and  $\mathbf{U}(t)$  is the nodal displacement vector. This leads to the following approximated strain field:

$$\boldsymbol{\varepsilon}(\mathbf{x}, t) = \frac{1}{2} \left( \nabla \mathbf{u}(\mathbf{x}, t) + (\nabla \mathbf{u}(\mathbf{x}, t))^T \right) = \mathbf{B}(\mathbf{x})\mathbf{U}(t) \quad (2)$$

where  $\nabla$  is the gradient operator and  $\mathbf{B}(\mathbf{x})$  is the discretized gradient matrix. After discretization, the equations of motion of an elastic structure in rotation are:

$$\mathbf{M}\ddot{\mathbf{U}} + \mathbf{G}\dot{\mathbf{U}} + (\mathbf{K} - \mathbf{K}_c)\mathbf{U} = \mathbf{F}_\Omega + \mathbf{F}_{ex} \quad (3)$$

where:

- $\mathbf{M} = \int_V \rho \mathbf{N}^T \mathbf{N} dV$  is the mass matrix

105

- $\mathbf{G} = 2 \int_V \rho \mathbf{N}^T \boldsymbol{\Omega} \mathbf{N} dV$  is the gyroscopic matrix
- $\mathbf{K} = \int_V \mathbf{B}^T \mathbf{C} \mathbf{B} dV$  is the stiffness matrix
- $\mathbf{K}_c = - \int_V \rho \mathbf{N}^T \boldsymbol{\Omega}^2 \mathbf{N} dV$  is the supplementary stiffness matrix
- $\mathbf{F}_\Omega = \int_V \rho \mathbf{N}^T \boldsymbol{\Omega}^2 \mathbf{x} dV$  is the nodal centrifugal force vector
- $\mathbf{F}_{ex}$  is the nodal external force vector.

with  $\rho$  the density,  $\mathbf{C}$  the elasticity matrix and  $\boldsymbol{\Omega}$  the rotation speed matrix:

$$\boldsymbol{\Omega} = \begin{bmatrix} 0 & -\Omega_z & \Omega_y \\ \Omega_z & 0 & -\Omega_x \\ -\Omega_y & \Omega_x & 0 \end{bmatrix} \quad (4)$$

Note that the gyroscopic matrix  $\mathbf{G}$ , the supplementary stiffness matrix  $\mathbf{K}_c$  and the nodal centrifugal force vector  $\mathbf{F}_\Omega$  all depend on the rotation speed. Considering the slenderness ratio of the structure and the range of rotation speeds investigated in this work, the effect of the gyroscopic matrix on the dynamic behavior of the rotating blade can be neglected [2, 11].

However, a geometric stiffness matrix depending of the nodal displacement vector,  $\mathbf{K}_g(\mathbf{U})$ , should be added to account for the centrifugal stiffening effects [12]:

$$\mathbf{M}\ddot{\mathbf{U}} + (\mathbf{K} - \mathbf{K}_c + \mathbf{K}_g(\mathbf{U})) \mathbf{U} = \mathbf{F}_\Omega + \mathbf{F}_{ex} \quad (5)$$

The solution of Equation (5) is performed in two steps [13].

The first step consists in solving the following non-linear static problem to determine the non-linear equilibrium position of the structure submitted to centrifugal forces  $\mathbf{U}^0$ :

$$(\mathbf{K} - \mathbf{K}_c + \mathbf{K}_g(\mathbf{U}^0)) \mathbf{U}^0 = \mathbf{F}_\Omega \quad (6)$$

The second step consists in linearising the dynamic problem around the nonlinear static equilibrium position, by assuming the dynamic displacement  $\mathbf{U}$  is a



small linear perturbation  $\mathbf{U}^*$  around the non-linear static equilibrium position  $\mathbf{U}^0$ :

$$\mathbf{U} = \mathbf{U}^0 + \mathbf{U}^* \quad (7)$$

Then Equation (5) becomes :

$$\mathbf{M}\ddot{\mathbf{U}}^* + (\mathbf{K} - \mathbf{K}_c + \mathbf{K}_g(\mathbf{U}^0)) \mathbf{U}^* = \mathbf{F}_{ex} \quad (8)$$

Under harmonic excitation, this dynamic system can be solved in the frequency domain :

$$(\mathbf{K} - \mathbf{K}_c + \mathbf{K}_g(\mathbf{U}^0) - \omega^2\mathbf{M}) \mathbf{U}^* = \mathbf{F}_{ex} \quad (9)$$

By incorporating viscoelastic materials into the structure, the stiffness matrix becomes complex, frequency and temperature dependent :

$$\mathbf{K}^*(\omega, T) = \mathbf{K}_e + G_1^*(\omega, T)\mathbf{K}_v^1 + G_2^*(\omega, T)\mathbf{K}_v^2 \quad (10)$$

110 where  $\mathbf{K}_e$  is the stiffness matrix associated to the elastic part of the structure,  $\mathbf{K}_v^1$  (resp.  $\mathbf{K}_v^2$ ) is the stiffness matrices associated to the viscoelastic material of the first patch (resp. second patch), and  $G_1^*(\omega, T)$  (resp.  $G_2^*(\omega, T)$ ) is the complex frequency and temperature dependent shear modulus of the viscoelastic material of the first patch (resp. second patch).

115 To sum up, the dynamic response of the blade-disk sector with viscoelastic patches to a harmonic load at a given rotation speed is computed in two steps :

- **Step 1** Computation of the non-linear static equilibrium position of the structure subjected to centrifugal forces  $\mathbf{U}^0$ :

$$(\mathbf{K}^*(0, T) - \mathbf{K}_c + \mathbf{K}_g(\mathbf{U}^0)) \mathbf{U}^0 = \mathbf{F}_\Omega \quad (11)$$

- **Step 2** Computation of the dynamic linear perturbation  $\mathbf{U}^*$  in the frequency domain:

$$(\mathbf{K}^*(\omega, T) - \mathbf{K}_c + \mathbf{K}_g(\mathbf{U}^0) - \omega^2\mathbf{M}) \mathbf{U}^* = \mathbf{F}_{ex} \quad (12)$$

Equation (11) can be solved by a Newton-Raphson method [13, 14], or an approximation of  $\mathbf{U}^0$  can be computed under small strain assumption [11]. The

latter approach is herein adopted. Considering the size of the finite element  
120 model, it is more efficient and has already been validated in a previous study  
by comparison with the Newton-Raphson approach. The model was built and  
the calculations made with an in-house software in Python, which has been val-  
idated by comparison with several commercial softwares.

To reduce the computational time, Equation (12) is solved by using a multi-  
125 modal projection method, which is adapted to structures with frequency-depen-  
dent damping [15].

### 3. Results and discussion

This section discusses the influence of operating conditions on the efficiency  
130 of viscoelastic damping treatment. The typical ranges of temperature and an-  
gular speed considered by engine manufacturers is  $[-40^{\circ}\text{C}, +70^{\circ}\text{C}]$  and  $[0, 2850]$   
RPM respectively. Following the dynamic modelling described in the previous  
section, frequency responses of the rotating blade disk sector with viscoelastic  
patches are computed at different operating points, under the assumption of  
135 stationary heating regime.

#### 3.1. Non-rotating case

In this section, the influence of temperature on the dynamic response of the  
non-rotating structure with viscoelastic patches is investigated. Figure 4 shows  
140 that a variation of temperature does not have a significant influence on the  
resonance frequencies of the structure. However, it has a strong influence on the  
amplitude of the dynamic response. Results also evidence a broad temperature  
range on which the damping treatment is efficient : from  $-10^{\circ}\text{C}$  to  $20^{\circ}\text{C}$ .  
The efficiency of viscoelastic patches depends on a number of parameters, such  
145 as the damping ratio of the viscoelastic material at a given temperature and  
frequency, the thickness ratio or the stiffness ratio between the core layer and

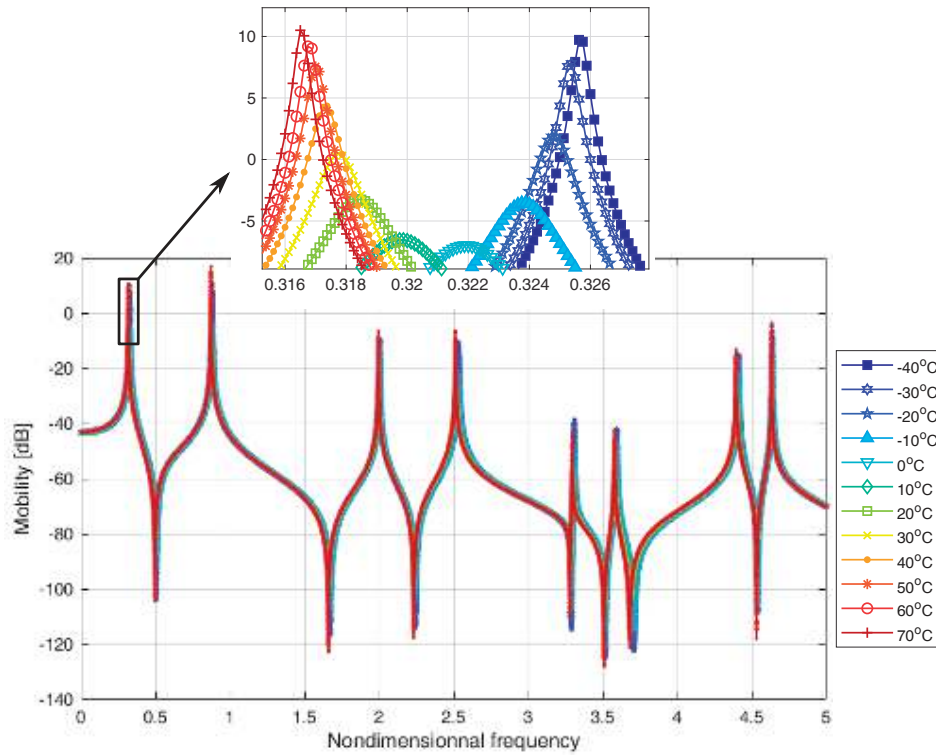


Figure 4: Influence of temperature on the dynamic response of the non-rotating structure with viscoelastic patches.

the elastic faces [16, 17]. In this work, the thickness ratio of both patches are the same, and the constraining layer of both patches are made of the same composite material. However, the viscoelastic material used as core layer in  
 150 both patches is different. The interest in combining two different viscoelastic materials for the patches will be discussed in Section 3.3.

### 3.2. Rotating case

In this section, the influence of the rotation speed on the efficiency of the damping treatment is investigated. To that purpose, the modal parameters of  
 155 the first six modes are extracted from the frequency responses using the LSCF method [18].

The modal parameters (resonance frequencies and modal damping) of the first vibration modes of the non-rotating and the rotating structure (2852 RPM) are plotted as a function of temperature in Figure 5 and 6. Figure 5 evidences the  
 160 well-known stress-stiffening effect : eigenfrequencies increase with the rotation

speed.

Figure 6 shows that the damping ratios are higher for the first mode of vibration, and more sensitive to a change of temperature or rotation speed. This is due to the fact that the viscoelastic patches have been designed to mainly damp the first vibration mode. For higher vibration modes, the viscoelastic layer undergoes less shear deformation, resulting in smaller damping ratios and less sensitivity to the parameters' variations under consideration. In particular, the damping ratios of the sixth mode are very small and are not affected by the rotation speed as the the sixth mode is a local vibration mode (see Figure 7). Some studies have shown that modal damping ratios generally decrease with increasing rotation speed [4]. This tendency is observed in Figure 6, regardless of the temperature. The decrease in modal damping ratio with increasing rotation speed is due to the stiffening effect, since the damping layer in the viscoelastic patches undergo less deformation. It should be noted that self-heating phenomena in the viscoelastic layers are not taken into account in this study. The amplitude of vibrations for this type of fan blade in operating conditions is considered small enough to neglect the temperature rise from the dissipation-induced self-heating.

### 3.3. Combining damping treatments

In the two previous sections, the viscoelastic material used as core layer in both patches is different. In this section, the interest in combining various damping materials for the patches is discussed. By comparing the master curves of the viscoelastic materials A and B in Figure 2, one can notice that they have distinct glass-rubber transition regions, characterised by a peak of loss factor and a drop in the storage modulus. The viscoelastic patches may then behave differently in temperature. This is investigated by studying three configurations:

1. **Configuration 1A-2B:** material A for the viscoelastic patch 1 and material B for the viscoelastic patch 2 (see Figure 1)
2. **Configurationn 1A-2A:** material A for both patches

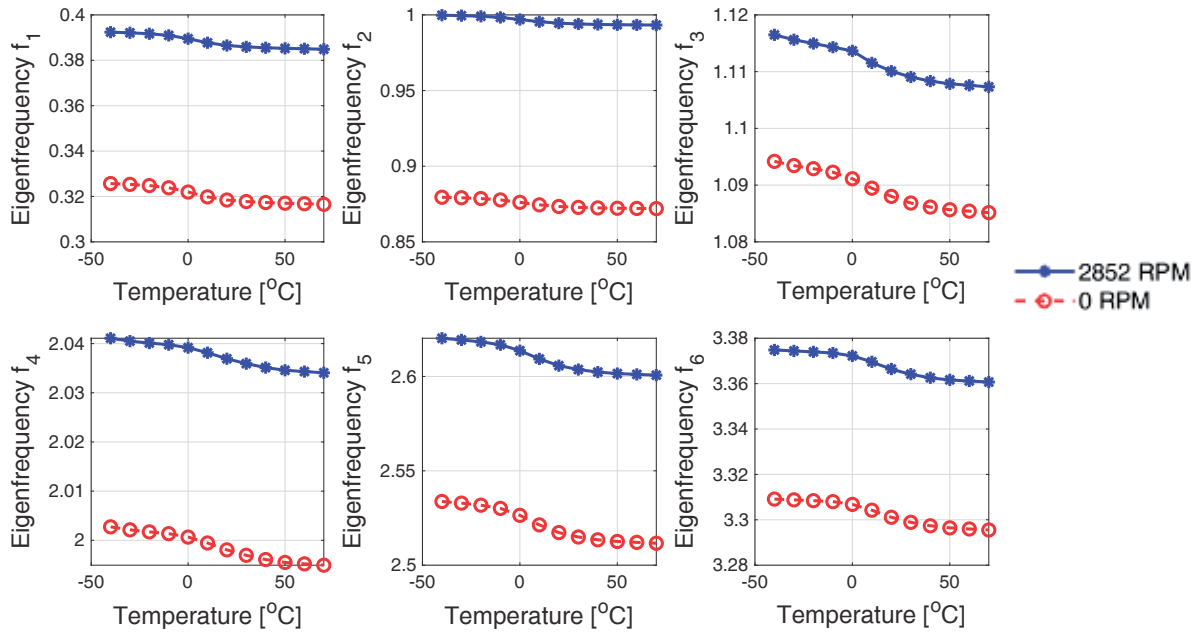


Figure 5: Influence of the rotation speed on the first resonance frequencies of the structure (frequencies are nondimensional).

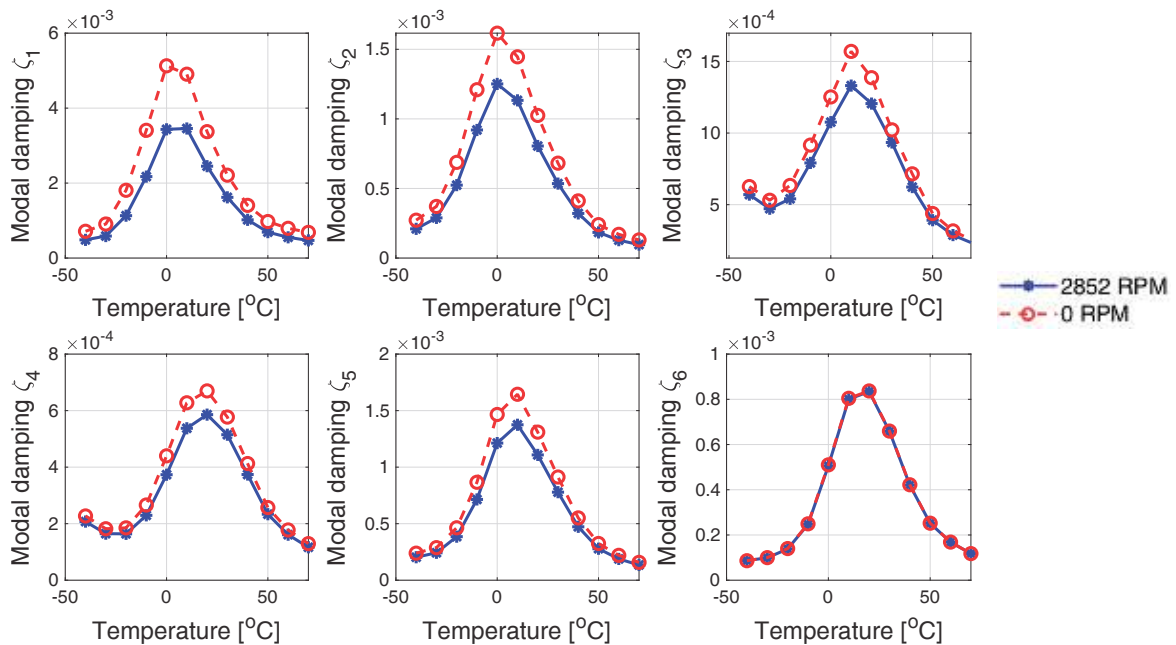


Figure 6: Influence of the rotation speed on the first modal damping ratios of the structure.

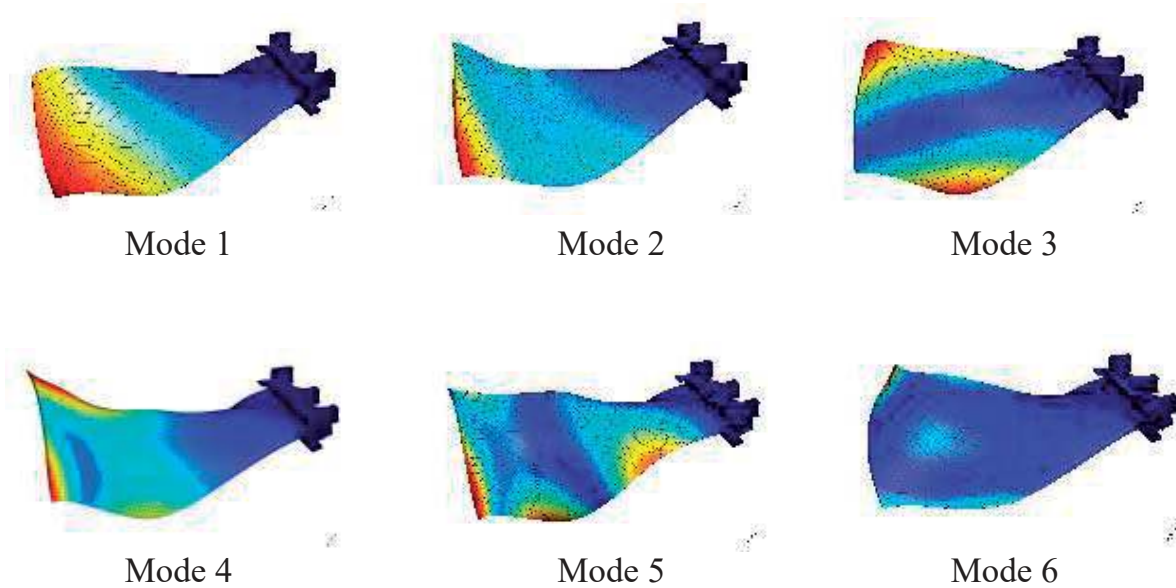


Figure 7: Unity-scaled mode shape of the first six vibration modes.

### 3. Configuration 1B-2B: material B for both patches

Figure 8 compares the modal damping factors of the first five modes extracted from FRF computations at 2852 RPM for the three configurations. Results indicate that material A is most efficient to damp vibration at lower temperatures (around  $0^{\circ}\text{C}$  for the first vibration mode) while material B is most efficient at higher temperatures (around  $15^{\circ}\text{C}$  for the first vibration mode). This can be related to the master curves from Figure 2, which indicate that material A has a lower glass transition temperature than material B. More importantly, combining two different damping treatments, as in configuration 1A-2B, allows a tuning of the temperature range of efficiency of the damping treatment. However, it does not seem to broaden the temperature range of efficiency.

## 4. Conclusion

In this work, a finite element model of a rotating composite fan disk sector with constrained viscoelastic patches is developed to predict the influence of temperature and rotation speed on the efficiency of the damping treatment. The frequency and the temperature dependency of viscoelastic materials are

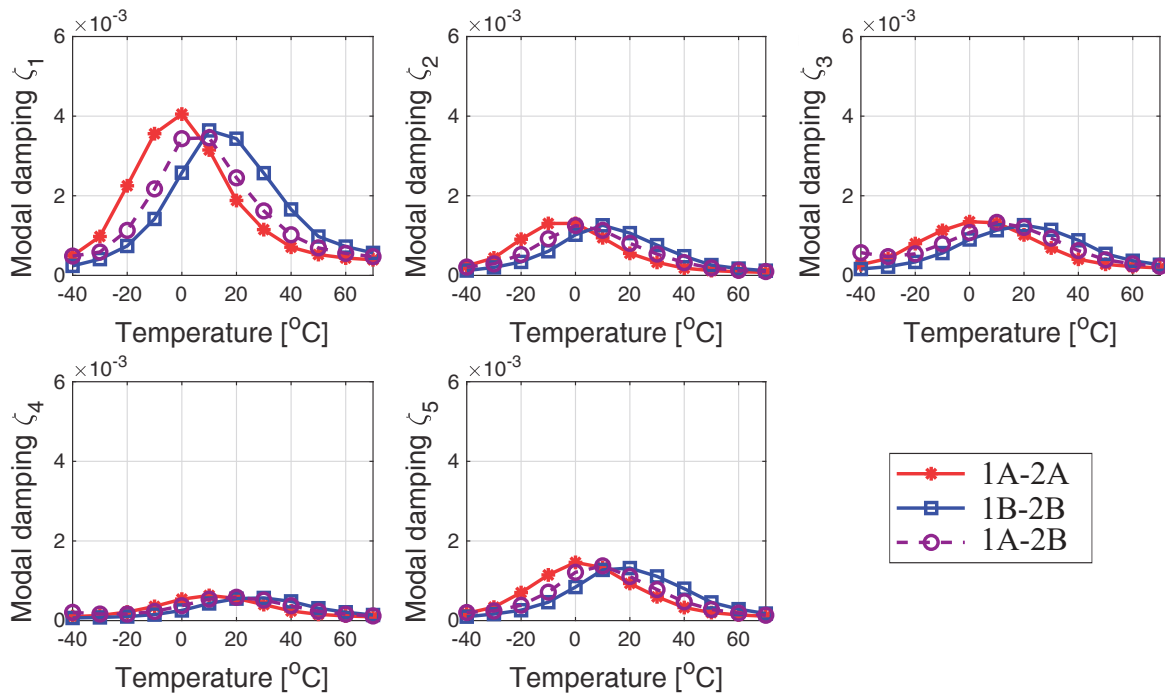


Figure 8: Modal damping ratios of the first five modes of the structure for three configurations. 1A-2A: material A used for both viscoelastic patches, 1B-2B: material A used for both viscoelastic patches, 1A-2B: material A for the viscoelastic patch 1 and material B for the viscoelastic patch 2.

taken into account and the multi-model projection method is used to compute the dynamic response of the rotating structure.

Results from frequency response analyses indicate that both temperature and rotation speed affect the modal damping ratios of the structure. The strong dependency of the mechanical properties of viscoelastic materials naturally implies that the damping treatment is efficient only on a reduced temperature range. This constitutes the main drawback of constrained viscoelastic patches. However, combining damping treatment made of different viscoelastic materials allows to tune temperature range of efficiency of the damping treatment.

It is also shown that modal damping ratios decrease when increasing the rotation speed, due to the stress stiffening effect. Moreover, the way modal damping ratios vary with temperature is not affected by the rotation speed. Therefore, for a given operating temperature range, appropriate viscoelastic materials can be chosen in the early design process without having to consider centrifugal effects.

## Acknowledgements

We gratefully acknowledge the collaboration and the financial support from SAFRAN group.

## References

- [1] Y.J. Kee, S.J. Shin, Structural dynamic modeling for rotating blades using three dimensional finite elements, *J. Mech. Sci. Technol.* 29 (2015) 1607–1618. <https://dx.doi.org/10.1007/s12206-015-0332-6>
- [2] Z. Shen, B. Chouvion, F. Thouverez, A. Beley, 2021. Enhanced 3D solid finite element formulation for rotor dynamics simulation. *Finite Elem. Anal. Des.* 195, 103584. <https://doi.org/10.1016/j.finel.2021.103584>



- 235 [3] Z. Xie, X. Xue, A new plate finite element model for rotating plate  
structures with constrained damping layer, *Finite Elem. Anal. Des.*  
47 (2011) 487–495. <https://doi.org/10.12691/jmdv-5-1-3>
- 240 [4] J. Sun, I. Lopez Arteaga, L. Kari, Dynamic modeling of a multilayer  
rotating blade via quadratic layerwise theory, *Compos. Struct.* 99  
(2013) 276–287. [https://doi.org/10.1016/j.compstruct.2012.  
12.012](https://doi.org/10.1016/j.compstruct.2012.12.012)
- [5] S. Na, J. Park, C.H. Park, M.K. Kwak, J.-H. Shim, Dynamic response  
analysis of rotating composite-VEM thin-walled beams incorporating  
viscoelastic materials in the time domain, *J. Mech. Sci. Technol.* 20(8)  
(2006) 1139–1148. <https://doi.org/10.1007/BF02916013>
- 245 [6] F. Boumediene, F. Bekhoucha, E.-M. Daya, Modal analysis of ro-  
tating viscoelastic sandwich beams, *Mech. Adv. Mater. Struct.* 28(4)  
405–417. <https://doi.org/10.1080/15376494.2019.1567887>
- [7] R.F. De Moura, P. Jean, S. Le Hong, J.-P. Lombard, 2013, Blade  
made of composite material comprising a damping device, US patent  
250 8 500 410. <https://patents.google.com/patent/US8500410> (ac-  
cessed 31 May 2022)
- [8] M. Ansar, W. Xinwei, Z. Chouwei, Modeling strategies of 3D woven  
composites: A review, *Comp. Struct.* 93(8) (2011) 1947–1963. <https://doi.org/10.1016/j.compstruct.2011.03.010>
- 255 [9] M. Krack, L. Salles, F. Thouverez, Vibration prediction of bladed  
disks coupled by friction joints, *Arch. Comput. Methods Eng.* 24  
(2017) 589–636. <https://doi.org/10.1007/s11831-016-9183-2>
- [10] MSC Software Corporation, MSC Nastran Rotordynamics User’s  
Guide, Version 20160, Newport Beach, Los Angeles, CA, 2016.
- 260 [11] D. Charleux, Etude des effets de la friction en pied d’aube sur la dy-  
namique des roues aubagées [Study of friction effects at the root of the

blade on the dynamics of bladed disks], Ph.D thesis, Ecole Centrale de Lyon (2006). <https://tel.archives-ouvertes.fr/tel-01130569>

- 265 [12] A. Vollan, L. Komzsik, Computational techniques of rotor dynamics with the finite element method, first ed., CRC Press, New York, 2012. <https://doi.org/10.1201/b11765>
- [13] G. Jacquet-Richardet, G. Ferraris, P. Rieutord, Frequencies and modes of rotating flexible bladed disc-shaft assemblies: a global cyclic symmetry approach, *J. Sound Vib.* 191(5) (1996) 901–915. <https://doi.org/10.1006/jsvi.1996.0162>
- 270 [14] S.H. Hsieh, J.F. Abel, Comparison of two finite element approaches for analysis of rotating-disk assemblies, *J. Sound Vib.* 182 (1995) 91–107. <https://doi.org/10.1006/jsvi.1995.0184>
- [15] L. Rouleau, J.-F. Deü, A. Legay, A comparison of model reduction techniques based in modal projection for structures with frequency-dependent damping, *Mech. Syst. Signal Process.* 90 (2017) 110–125. <https://doi.org/10.1016/j.ymssp.2016.12.013>
- 275 [16] B.R. Sher, R.A.S. Moreira, Dimensionless analysis of constrained damping treatments, *Compos. Struct.* 99 (2013) 241–254. <https://doi.org/10.1016/j.compstruct.2012.11.037>
- 280 [17] M. Gröhlich, M. Böswald, R. Winter, 2019, Vibration damping capabilities of treatments with frequency and temperature dependent viscoelastic material properties, Proceedings of the 23rd International Congress on Acoustics: integrating 4th EAA Euroregio 2019, Aachen, Germany. <http://dx.doi.org/10.18154/RWTH-CONV-239254>
- 285 [18] M. El-Kafafy, P. Guillaume, B. Peeters, F. Marra, G. Coppotelli, Advanced frequency-domain modal analysis for dealing with measurement noise and parameter uncertainty, in: R. Allemang, J. De Clerck, C. Niezrecki, J. Blough (Eds.), *Topics in Modal Analysis I*,

Volume 5, Springer, New York, 2012, 179–199. [https://doi.org/10.1007/978-1-4614-2425-3\\_17](https://doi.org/10.1007/978-1-4614-2425-3_17)